BIOCHEMISTRY
including biophysical chemistry & molecular biology

Article

pubs.acs.org/biochemistry

Effect of Cholesterol on the Membrane Interaction of Modelin-5 Isoforms

Sarah R. Dennison[†] and David A. Phoenix*[,‡]

[†]School of Pharmacy and Biomedical Sciences, University of Central Lancashire, Preston PR1 2HE, U.K.

[‡]Office of the Vice Chancellor, University of Central Lancashire, Preston PR1 2HE, U.K.

ABSTRACT: Modelin-5 isoforms were used to gain an insight into the effects of amidation on antimicrobial selectivity. When tested against *Escherichia coli*, amidation increased toxicity 10-fold (MIC = 31.25 μM) while showing limited increased hemolytic activity (2% lysis). Our results show that both the amidated and non-amidated peptides had a disordered structure in aqueous solution (<18% helical) and folded to form helices at the membrane interface (for example, >43% in the presence of DMPC). The stabilization of the helical structure by amidation has previously been shown to play a key role in increasing antibacterial efficacy. The presence of cholesterol in the membrane increases the packing density (C_s^{-1} values 25−33 mN m^{-1}) and so prevents the peptide from forming stable association with the membrane, which is evidenced by the higher binding coefficient (K_d) in the presence of cholesterol: 57.70 μM for Modelin-5-COOH and 35.64 μM for Modelin-5-CONH$_2$ compared to the presence of *E. coli* lipid extract (10 μM), which would prevent local concentration of the peptide at the bilayer interface as seen by reduction in monolayer interaction. This in turn would be predicted to inhibit activity.

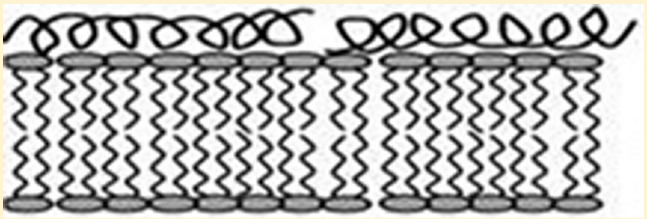

The incidence of bacterial infection during blood transfusion is much higher than other transfusion-transmitted infections such as HIV[1−3] and still remains an unresolved problem in transfusion medicine with bacterial contamination estimated between 1 and 30 000 red blood cell (RBC) units.[1] Although donated blood is screened for micro-organisms, which could lead to transfusional transmission of disease,[4,5] there are many challenges to overcome in order to destroy the bacterial cells which cause infection, and a number of new interventions have been suggested to help address issues of blood contaminants. For example, γ-irradiation is a technique used to clean blood from bacterial infection; however, not all bacterial growth is prevented using this technique.[6] More recently, photochemicals such as methylene blue derivatives have been seen as providing a more promising approach to inactivation of a wide range of bacterial species[7] although Harris et al.[8] reported that while these compounds had the potential for further development, the hemolytic effects of photosynthetic dyes (6−19%) were still problematic. Indeed, a key challenge remains the identification of antimicrobial agents which are able to target micro-organisms without causing hemolysis.[5,7]

More recently, antimicrobial peptides (AMPs) have generated considerable interest as a design template for potential antibiotics.[9] AMPs can be classified into two groups: those which are cell selective or alternatively non-cell selective[10] and would have potential for use in blood decontamination if selectivity for bacterial cells over erythrocytes could be enhanced. Bessalle et al.[11] used quantitative structure−activity relationships (QSAR) of AMPs to design a family of novel synthetic AMPs termed Modelins. In comparison to other Modelins, Modelin-5-COOH (KLAKKLAKLAKLAKAL-COOH) was seen to have potent cidal action against a wide variety of Gram-positive and Gram-negative bacteria but relatively low hemolytic activity. Furthermore, studies have shown that C-terminal amidation enhances Modelin-5 peptide structure stability and so increases the efficacy of the peptide as an antimicrobial agent.[9,12] Such post-translational modifications could therefore increase the potential of AMPs to be used in blood decontamination if they do not generate a concomitant increase in hemolysis. It would therefore be useful to understand the impact of this modification on cell selectivity.

Almost all AMPs are amphiphilic, although their final fold varies depending on the membrane composition.[13] For example, the bee venom, melittin, which is known to be a non-cell selective lytic peptide, shows varying levels of antimicrobial activity among bacterial species,[14] and this is thought to be due to variation in the phospholipid composition of the target membrane and the packing characteristics of the lipid acyl chains. Furthermore, researchers have shown that the efficacy of potential anticancer AMPs is effected by the variation in phospholipid content of eukaryotic cells.[15,16] In general, the outer membrane leaflet of mammalian erythrocytes is mainly composed of phosphatidylcholine (PC) and sphingomyelin (SM) although the PC to SM ratio varies considerably.[17,18] Other phospholipids, phosphatidylethanolamine (PE), phosphatidylinositol (PI), phosphatidylserine

Received: August 11, 2011
Revised: November 14, 2011
Published: November 14, 2011

(PS), and lysophosphatidylcholine are also present in the membrane of mammalian erythrocytes.[17] Given this eukaryotic membrane lipid composition[19] shows variation to prokaryotic systems, this would support the view that selectivity could be increased.

A major difference between bacterial and mammalian membranes is the presence of cholesterol in the membrane. Cholesterol is a major component of erythrocytes membranes comprising 27% of total membrane lipid,[20] and its absence in bacterial membranes may underlie the difference in selectivity of the AMP for bacterial cells over erythrocytes. A number of researchers have suggested that cholesterol reduces the ability of some AMPs to associate with the membrane[21−25] and that it protects the host cell from membrane permeabilization.[22,23] For example, Zhao and Kinnunen[23] showed that the insertion of an amphibian AMP Temporin L was inhibited in the presence of cholesterol and proposed either a "toroidal" or "barrel stave" model of membrane interaction. Indeed, cholesterol is also known to decrease the in-plane elasticity of PC and sphingomyelin monolayers,[21,26] and high levels of cholesterol have pronounced effects on the physical properties of the bilayer. It is suggested that the augmented lipid packing required to accommodate the sterol ring structure within the headgroup region could prevent the interaction of the AMPs and hence cholesterol may protect the host cell from membrane disruption from the AMP.[22,27] Indeed, Monette et al.[28] proposed that the presence of cholesterol prevented the penetration of melittin into 1,2-dipalmitoyl-*sn*-glycero-3-phosphocholine/cholesterol mixtures because of the tight phospholipid packing of the membrane induced by cholesterol, and further research undertaken by Gomara et al.[29] showed that the presence of cholesterol did indeed reduced the efficiency of melittin pore formation. Although a number of studies on the interactions of AMPs with phospholipids have been undertaken, very few studies have been undertaken into the effect of cholesterol on the membrane interactions of amidated AMPs. In the present study the effect of cholesterol on cell lysis was investigated using amidated and nonamidated isoforms of Modelin-5 in an attempt to understand key determinants of efficacy against bacterial cells verses erythrocytes.

EXPERIMENTAL PROCEDURES

Materials. Lipids were obtained from Avanti, and peptides Modelin-5-COOH and Modelin-5-$CONH_2$ were from Pepceuticals (Leicestershire, UK); all were used as supplied. All buffers were prepared using ultrapure water (resistivity 18 MΩ cm). Solvents were obtained from VWR (HPLC grade), and all other regents were purchased from SIGMA-Aldrich (UK).

Hemolysis Assay. 3 mL of fresh pig red blood cells were washed 3 times with PBS (35 mM phosphate buffered saline, 0.15 M NaCl, pH 7.4) by centrifugation for 5 min at 1200*g* until the supernatant was clear. Washed red blood cells were resuspended in PBS to a final volume of 20 mL. The peptide solutions (10 μL) were added to 190 μL suspension of washed red blood cells and were incubated for 1 h at 37 °C. The samples were then centrifuged at 12000*g* for 5 min. The release of hemoglobin was monitored by diluting 100 μL of supernatant with 900 μL of PBS and absorbance measured at 576 nm. For negative and positive controls, PBS buffer [A_{PBS}] and 0.1% Triton X-100 [A_{Triton}] were used. The percentage hemolysis was calculated according to the equation[30,31]

$$\%\ \text{hemolysis} = \frac{[A_{peptide}] - [A_{PBS}]}{[A_{Triton}] - [A_{PBS}]} \times 100 \quad (1)$$

Total Lipid Extracts from Cells of *E. coli* and Pig Erythrocytes. A modified protocol of the Bligh and Dyer[32] method of lipid extraction was used to extract *E. coli* and pig erythrocyte membrane lipids. In summary, cultures of *E. coli* were grown in nutrient broth until exponential phase (OD = 0.6; λ = 600 nm) and then washed twice in 1/4 strength Ringers and centrifuged using a Jouran benchtop centrifuge at 14 000 rpm to form a cell pellet. The pig erythrocytes were prepared according to Rose and Oklander.[33] In summary, fresh pig red blood cells were washed 4 times in cold buffer (145 mM NaCl, 5 mM KCl, 5 mM HEPES, pH 7.4), at 4 °C and centrifuged 10 min at 2000*g*. The cells were lysed using cold hypotonic buffer containing 15 mM KCl, 0.01 mM EDTA, 1 mM EGTA, 5 mM Hepes, pH 6.0. The cell suspension was centrifuged for 10 min at 4 °C and 12000*g*. The cell pellet was washed with 15 mM KCl, 0.01 mM EDTA, and 5 mM Hepes and then centrifuged for a further 10 min at 4 °C and 12000*g*. Bacteria and erythrocyte cell pellets were resuspended in 1 mL of Tris buffer (10 mM, pH 7.5), and to a 0.4 mL aliquot of this cell suspension, 1.5 mL of a 1:2 (v/v) chloroform−methanol mixture was added and then vortexed. 0.5 mL of water was then added and vortexed for 5 min before being centrifuged at low speed (660*g*, 5 min) to produce two phases. The lower organic layer was concentrated using a Jouran speed vac (Jouran, UK), and the dried lipid extract was stored at −20 °C under N_2.

Circular Dichroism Measurements. Peptides (0.1 mg mL^{-1}) were dissolved in PBS or small unilamellar vesicle (SUVs) suspensions to maintain a peptide to lipid ratio of 1:100. To obtain the SUVs, a predetermined amount of dried (5 mg/mL) DMPE, DMPC, DMPC, *E. coli* lipid extract, pig blood lipid extract, or cholesterol:DMPE/PC (molar ratios 0.1, 0.25, 0.33, 0.5, and 0.87) were dissolved in chloroform, evaporated under a stream of nitrogen, placed under vacuum for 4 h, and rehydrated using PBS pH 7.5. The suspension was vortexed for 5 min before sonicated for 30 min, and the solution underwent three cycles of freeze−thawing. Liposomes were then extruded 11 times through a 0.1 μm polycarbonate filter using an Avanti Polar Lipids Mini-Extruder apparatus. All CD experiments were obtained by acquiring 10 scans on a J-815 spectropolarimeter (Jasco, UK) using a 10 mm path-length cell over a wavelength range 260 to 180 at 100 nm/min, 1 nm bandwidth, data pitch 0.5 nm, and samples maintained at 20 °C. For all spectra acquired, the baseline acquired in the absence of peptide was subtracted.[34] The percentage helical content was estimated using a method previously described by Forood et al.[35] These experiments were repeated four times, and the percentage helicity was averaged. To determine whether there was a statistically significant difference between the percentage helicity of the two peptides in the presence of each phospholipid PC and PE, a T-test was undertaken, using SPSS v 19, based on the null hypothesis that there was no difference between the mean percentage helicity. An ANOVA was also undertaken to determine whether there was a significant difference in the percentage helicity for the phospholipid cholesterol mixes, based on the null hypothesis that there was no significant difference in the helicity levels.

Monolayer Experiments. Insertion experiments were carried out at constant area to quantify the interaction of the peptide isoforms with phospholipid monolayers using a 601 M

Langmuir Teflon trough (Biolin Scientific\KSV NIMA, Coventry, UK). All monolayer experiments were undertaken at 20 °C. *E. coli* and pig blood lipid extract and phospholipid stock solutions (1 mg mL^{-1}) of cholesterol:PC and of cholesterol:PE in chloroform were prepared at the following cholesterol:PC/PE ratios 0, 0.1, 0.25, 0.33, 0.5, and 0.87 and were spread dropwise onto an air−buffer (10 mM Tris, pH 7.4) interface using a Hamilton microsyringe. The solvent was allowed to evaporate off, and then the monolayer was compressed by two moveable Derlin barriers with a velocity of 50 mm/min to a starting surface pressure of 30 mN m^{-1}, which corresponds to the packing density of a cell membrane.[36,37] The surface area was kept constant via a built-in controlled feedback system. The Modelin-5 peptide solution was injected underneath the monolayer using an L-shaped needle syringe to give a final peptide concentration of 6 μM in the subphase. Surface pressure increases were monitored by the Wilhelmy method using a Whatman's CH1 filter paper plate and microbalance.[38] To determine whether there was a statistically significant difference between the surface pressure changes and phospholipid cholesterol mixes, an ANOVA was undertaken using SPSS v 19, based on the null hypothesis that there was no difference between the mean surface pressure changes. Regression analysis was also undertaken to identify the correlation between surface pressure change and cholesterol phospholipid ratio.

Compression isotherms of cholesterol:PC ratios 0.05 and 0.1 were formed by spreading 2.5×10^{15} phospholipid molecules onto a 10 mM Tris buffer subphase. The lipid monolayers were allowed to settle for 30 min before compression of the barriers at a speed of 0.22 nm^2 min^{-1} until monolayer collapse pressure was achieved. These experiments were then repeated in the presence of either 6 μM Modelin-5-COOH or Modelin-5-$CONH_2$. Compressibility modulus (C_s^{-1}) at each of the experimental mixing ratios were calculated by applying the equation[39]

$$C_s^{-1} = -A\left(\frac{\delta\pi}{\delta A}\right) \tag{2}$$

where A is the area per molecule at a given surface pressure (π).

Using the isotherms determined, the thermodynamic stability of monolayers was then investigated by applying the Gibbs equation:

$$\Delta G_{mix} = \int A_{12} - (X_1A_1 + X_2A_2)\, d\pi \tag{3}$$

where $A_{1,2,...}$ is the molecular area occupied by the mixed monolayer, A_1, A_2, are the area per molecule in the pure monolayers of component 1, 2; X_1, X_2 are the molar fractions of the components, and π is the surface pressure. Numerical data were calculated from the compression isotherms according to the mathematical method of Simpson.[40]

Calcein Leakage Assay. For this assay eight different model cell membranes were used: *E. coli* model (1 PG:13.6 PE:2 CL), pig blood model (1PE:6 PS:7.4 SM:11.1 PC:10.44 PE[19]), DMPE, DMPC, and cholesterol:DMPC (molar ratios 0.1, 0.25, 0.33, 0.5, and 0.87). Unilamellar vesicles were prepared by dissolving 7.5 mg of phospholipid in chloroform and dried under a stream of nitrogen. The sample was kept under vacuum for at least 12 h to ensure complete removal of the solvent. The lipid film was then hydrated with 1 mL of 5.0 mM HEPES containing 70 mM calcein. The suspension was vortexed for 5 min before sonicated for 30 min. The solution then underwent three cycles of freeze−thawing to maximize the calcein encapsulation. Liposomes were extruded 11 times through a 0.1 μm polycarbonate filter using an Avanti Polar Lipids Mini-Extruder apparatus. Calcein entrapped vesicles were separated from free calcein by gel filtration using a Sephadex G75 column (Sigma) which was rehydrated overnight in 20 mM HEPES, 150 mM NaCl, and 1.0 mM EDTA. The column was eluted with 5 mM HEPES, pH 7.5.

The calcein release assay was performed at 20 °C by combining 2 mL of 20 mM HEPES, 150 mM NaCl, and 1.0 mM EDTA (pH 7.4) and 20 μL of calcein vesicles. The fluorescence intensities of calcein was measured using a FP-6500 spectrofluorometer (JASCO, Tokyo Japan), with an excitation wavelength of 490 nm and an emission wavelength of 520 nm. To measure maximum fluorescence, 20 μL of Triton X100 was used to dissolve the vesicles. The percentage of dye leakage was then calculated. To determine whether there was a statistically significant difference between the calcein leakage of the two peptides in the presence of each phospholipid mix, a T-test was undertaken, using SPSS v 19, based on the null hypothesis that there was no difference between the mean calcein leakage. Further statistical analysis was undertaken to investigate the differences between calcein leakage and the phospholipid cholesterol mixes using an ANOVA based on the null hypothesis that there was no difference between the mean calcein leakage.

To investigate the effects of temperature, the experiments were repeated using DMPC, DMPE, and 0.89 cholesterol:PC/PE at 25, 50, and 55 °C. Statistical analysis based on the null hypothesis that there was difference between the mean calcein leakage across the temperature range tested was undertaken using an ANOVA test.

Peptide Binding to Vesicles. Unilamellar vesicles with a mean diameter of 0.1 μm were prepared as previously described by Wall et al.[41] Phospholipid cholesterol:PE ratios were prepared as before, and 0.5 mol % of fluorescein−phosphatidylethanolamine (FPE) was added to the organic solvent before drying under vacuum for 5 h. The lipids were hydrated in 10 mM Tris-HCl pH 7.4; 1 mM EDTA at a total lipid concentration 10 mg mL^{-1}, freeze−thawed five times and extruded 11 times using a 0.1 μm polycarbonate filter using an Avanti Mini-Extruder apparatus. FPE-labeled vesicles were diluted to 65 μM, and fluorescence was recorded using a FP-6500 spectrofluorometer (JASCO, Tokyo Japan), with an excitation wavelength of 492 nm and an emission wavelength of 516 nm. The incorporation of the FPE label was checked using the methodology previously described by Wall et al.[41] To investigate the binding peptide to the varying cholesterol:PE ratios, aliquots of each peptide (range 0−320 μM) were added to the FPE-labeled vesicles and the fluorescence was monitored. The change in fluorescence (ΔF) of FPE-labeled vesicles with addition of peptide minus FPE-labeled vesicles was plotted against peptide concentration and fitted by nonlinear least-squares analysis to

$$\Delta F = \frac{\Delta F_{max}[M]}{K_d + [M]} \tag{4}$$

where [M] is the Modelin concentration, ΔF the fluorescence change, F_{max} the maximum fluorescence change, and K_d the binding constant.

To determine whether there was a statistically significant difference between the binding constant of the two peptides in the presence of each phospholipid mix, a T-test was undertaken, using SPSS v 19, based on the null hypothesis that there was no difference between the mean binding constants.

RESULTS

Antimicrobial Activities of Modelin-5. Modelin-5 isoforms exhibited antimicrobial activity against *E. coli* with a minimum inhibitory concentration (MIC) of 250 μM (Modelin-5-COOH) and 31.25 μM (Modelin-5-$CONH_2$), respectively, which is in line with previous studies.[9] Since Modelin-5-COOH was orignially designed by Bessalle et al.[11] to exhibit reduced hemolytic activity, both peptides were tested against pig blood. Figure 1 shows even though amidation

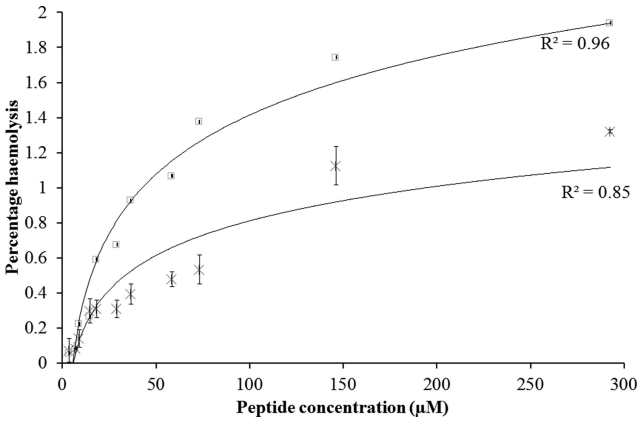

Figure 1. Percentage haemolysis of pig red blood cells at different peptide concentrations for Modelin-5-COOH (×) and Modelin-5-$CONH_2$ (□) where $n = 4$ with error shown by standard deviations.

enhanced hemolysis, both peptides have low hemolytic activity (<2%) at peptide concentrations up to 300 μM (Figure 1), which correlates to previously published work by Owen,[42] who reported that at peptide concentrations <200 μg/mL (58.55 μM) Modelin-5-COOH induced 2% hemolysis of human red blood cells.

Secondary Structure of Modelin Peptides. Secondary structure analysis was performed using CD spectral data. Previous studies have shown that Modelin-5-COOH adopted an unordered structure in aqueous solution;[11] however, the presence of 50% TFE induced 52% α-helical structure.[11] In order to investigate whether these peptides remained in an α-helical structure in different lipid environments, CD experiments were undertaken in the presence of vesicles with differing membrane lipid compositions.

Figure 2 shows the solution CD spectra from Modelin-5 isoforms in the presence of buffer or vesicles formed from pig blood lipid extract, *E.* coli lipid extract, DMPE, or DMPC. The CD spectra of Modelin-5-COOH and Modelin-5-$CONH_2$ in PBS buffer showed an unordered structure (13% and 18% helicity, respectively; Table 1), and statistical analysis indicated a significant difference in helicity between the two Modelin-5 isoforms [$T = -9.46$; $p = 0.03$]. In the presence of liposomes enhanced helicity was observed for both peptides. The results showed that in the presence of *E. coli* lipid extract amidation enhanced helicity to 32% (Modelin-5-COOH) or 69% (Modelin-5-$CONH_2$), respectively, thereby showing a the

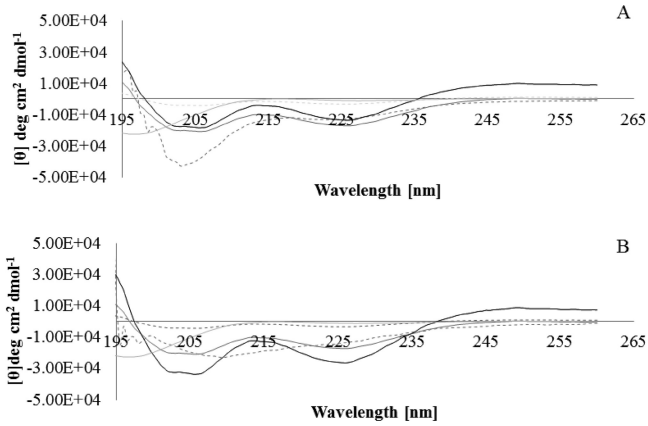

Figure 2. CD spectra of (A) Modelin-5-COOH and (B) in Modelin-5-$CONH_2$ in the presence of aqueous solution (dotted light gray), *E. coli* extract (solid black), pig extract (solid light gray), DMPC (dotted black), and DMPE (dotted dark gray).

Table 1. Percentage Helicity and Percentage Calcein Leakage of Modelin-5- COOH and Modelin-5-$CONH_2$

	% helicity and standard deviation		% leakage and standard deviation	
membrane composition	Modelin-5-COOH	Modelin-5-$CONH_2$	Modelin-5-COOH	Modelin-5-$CONH_2$
solution (PBS)	13 ± 0.4	18 ± 0.8		
DMPC	43 ± 1.7	45 ± 0.5	43 ± 3.5	47.1 ± 2.4
DMPE	44 ± 0.71	45 ± 0.6	35 ± 1.0	39 ± 1.0
pig blood lipid extract	25 ± 0.5	26 ± 0.6	0.72 ± 0.01	2.6 ± 0.4
E. coli lipid extract	32 ± 0.8	69 ± 0.6	42 ± 1.7	74 ± 1.5

lipid interface generated much greater level of helicity in the case of the amidated isoform [$T = -123.33$; $p = 0.00$] (Table 1). The CD spectra in Figure 2 show minima at 221−222 and 209−210 nm and a maximum at about195 nm for both peptides, which is characteristic of α-helical structure. However, in the presence of pig blood lipid extract, the CD spectra show that the α-helical characteristics are reduced, indicating that reduced helicity was observed for both Modelin-5-COOH (25%) and Modelin-5-$CONH_2$ (26% helical) compared to levels in the presence of bacterial extract, and in this case amidation did not lead to enhanced helicity. The ability of Modelin-5 isoforms to form α-helical structure in the presence of cholesterol was investigated (Figures 3 and 4) in conjunction with either eukaryotic PC or PE, a zwitterionic lipid found in both prokaryotic and eukaryotic membranes. No significant differences were observed between the levels of helicity induced in either the nonamidated or amidated isoforms in the presence of PC or PE alone [$T = -2.307$; $p = 0.10$].

Figure 3A shows that in the presence of cholesterol:PC ratios of 0.1 the Modelin-5-COOH CD spectra display a double minima at 208 and 222 nm, and further spectra analysis indicated that Modelin-5-COOH adopted a 32% helical conformation. However, increasing cholesterol levels showed a linear correlation with decreased helicity down to 6% ($R^2 = 0.93$) at ratios found within pig erythrocyte lipid extract (0.87; Figure 4A). Statistical analysis confirmed that increased cholesterol induced a significant difference in the percentage helicity [$F_{1,23} = 966.70$; $p = 0.00$]. In the presence of cholesterol:PE (Figure 4B) the helical content also decreased

dx.doi.org/10.1021/bi201267v | *Biochemistry* 2011, 50, 10898−10909

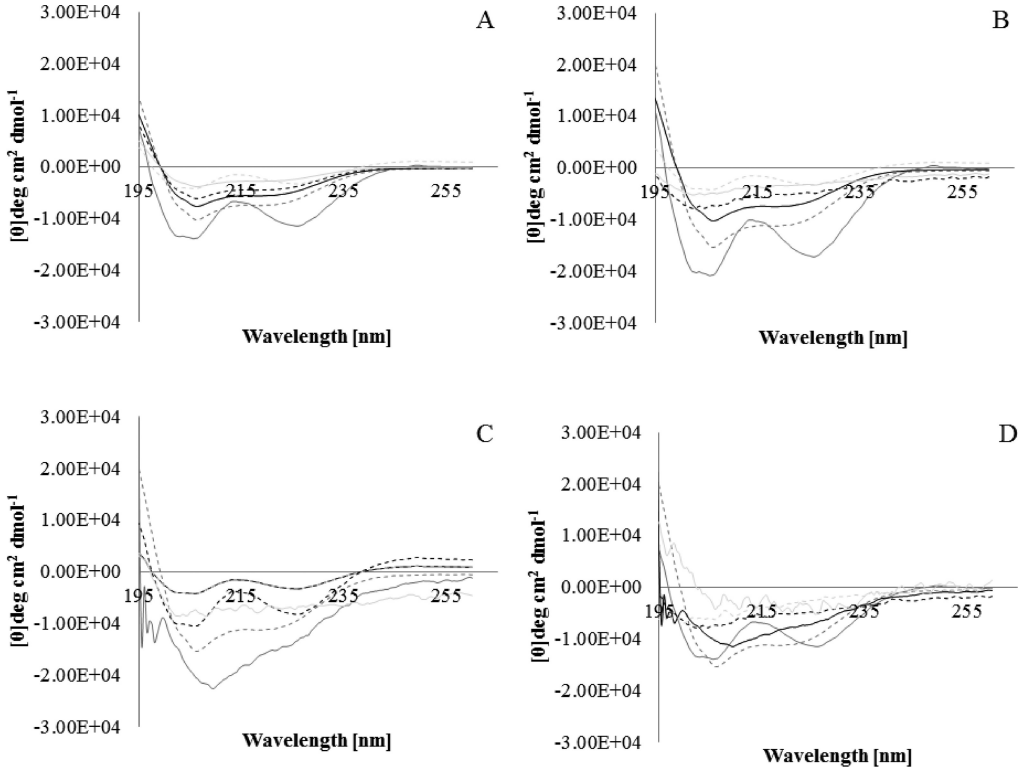

Figure 3. CD spectra (A) of Modelin-5-COOH in the presence of DMPC (solid dark gray), cholesterol:PC ratios 0.1 (dashed gray), 0.25 (solid black), 0.33 (dashed black), 0.5 (solid light gray), and 0.87 (dashed light gray); (B) of Modelin-5-$CONH_2$ in the presence of DMPC (solid dark gray), cholesterol:PC ratios 0.1 (dashed gray), 0.25 (solid black), 0.33 (dashed black), 0.5 (solid light gray), and 0.87 (dashed light gray); (C) of Modelin-5-COOH in the presence of DMPE (solid dark gray), cholesterol:PE ratios 0.1 (dashed gray), 0.25 (solid black), 0.33 (dashed black), 0.5 (solid light gray), and 0.87 (dashed light gray); (D) of Modelin-5-$CONH_2$ in the presence of DMPE (solid dark gray), cholesterol:PE ratios 0.1 (dashed gray), 0.25 (solid black), 0.33 (dashed black), 0.5 (solid light gray), and 0.87 (dashed light gray).

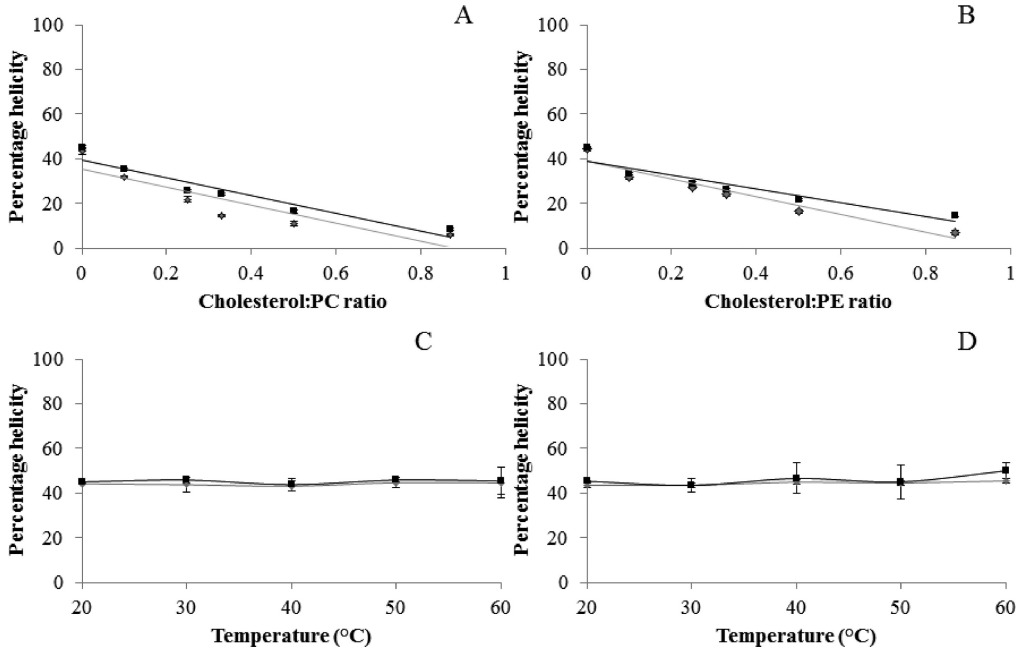

Figure 4. Percentage helicity of Modelin-5-COOH (gray) and Modelin-5-$CONH_2$ (black) for $n = 4$ and with error bars showing standard deviations: (A) in the presence of cholesterol:PC; (B) in the presence of cholesterol:PE; (C) the effects of temperature in the presence of PC. Statistical analysis showed there was no significant difference in percentage helicity of Modelin-5-COOH [$F_{4,9} = 0.93$; $p = 0.52$] and Modelin-5-$CONH_2$ [$F_{4,9} = 0.48$; $p = 0.75$]. (D) Effects of temperature in the presence of PE. Statistical analysis showed there was no significant difference in percentage helicity for both Modelin-5-COOH [$F_{4,9} = 0.06$; $p = 0.99$] and Modelin-5-$CONH_2$ [$F_{4,9} = 0.16$; $p = 0.95$].

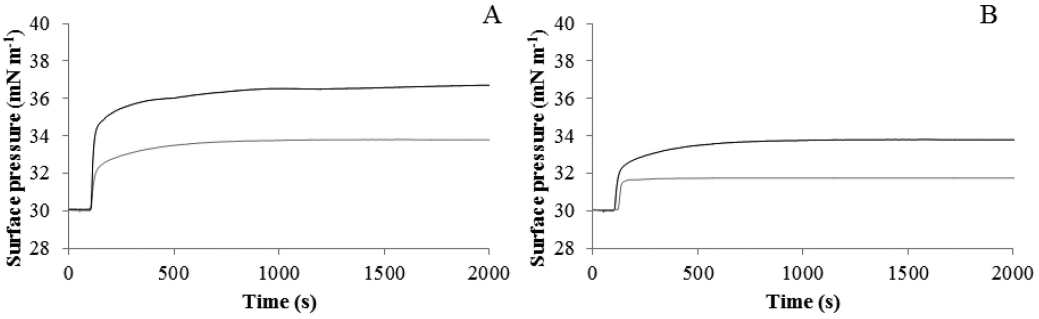

Figure 5. Time course of Modelin-5-COOH (gray) and Modelin-5-$CONH_2$ (black) with *E. coli* (A) and pig erythrocyte (B) lipid extract monolayers.

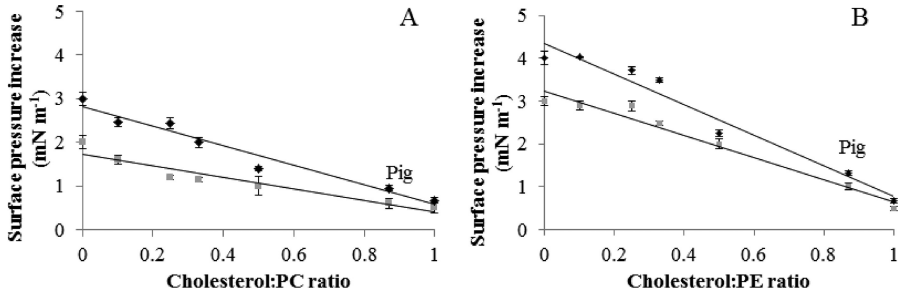

Figure 6. Effect of varying cholesterol levels in monolayers on the levels of interaction shown by Modelin-5-COOH (gray) and Modelin-5-$CONH_2$ (black) with PC (A) and PE (B). Error bars are standard deviations.

from 32% to 6% as the cholesterol:PE ratio levels increased to that seen in the pigs blood lipid extract (R^2 = 0.91), and ANOVA again confirmed that there was a significant difference in helicity with increased cholesterol levels [$F_{1,23}$ = 995.43; p = 0.00]. CD spectral changes indicated not only reduced helicity but also an increase in random coil and β-sheet conformation with increasing cholesterol levels (Figure 3). The presence of cholesterol:PE and cholesterol:PC showed no significant variations in the level of helicity induced for Modelin-5-COOH [T = 2.46; p = 0.57] or Modelin-5-$CONH_2$ [T = 1.85; p = 0.123] by the two lipid systems, indicating no evidence for preferential binding to either lipid.

Figure 4C,D shows the change in Modelin-5-COOH and Modelin-5-$CONH_2$ helical content over the temperature range 20−60 °C in the presence of DMPC or DMPE. In the presence of DMPC (Figure 4C), as the temperature increases above the lipid phase transition temperature of 23 °C,[43] there is a slight decrease in helical content for both peptide isoforms, but this is not statistically significant (p > 0.05) over the temperature range investigated. In the case of DMPE, where the lipid phase transition temperature is 50 °C,[43] Figure 4D shows that there is again no significant change in helicity (p > 0.05) over the temperature range 20−60 °C for either peptide. Overall, these results suggest that both Modelin-5 isoforms are able to form stable peptide structure at a membrane interface, and this is not influenced by the phase transition temperature of these two lipids.

Monolayer Interactions of Modelin-5. One of the most important stages of peptide−membrane interaction is the initial contact between the peptide and the outer leaflet of the membrane. The insertion of Modelin-5-$CONH_2$ into *E. coli* (Figure 5A) and pig blood (Figure 5B) lipid extract monolayers followed hyperbolic kinetics inducing surface pressure changes of 6.1 and 3.78 mN m^{-1}, respectively. The high levels of interaction for Modelin-5-$CONH_2$ with *E. coli* membranes is consistent with disruption of the monolayer acyl chain region; however, the presence of erythrocyte lipid extract clearly inhibited binding and/or insertion. Modelin-5-COOH was also able to interact with *E. coli* and pig blood lipid extract, but the peptide induced significantly lower surface pressure changes of only 4 and 1.60 mN m^{-1}, respectively, implying it is less able to penetrate into the acyl chain region.

It is well established that cholesterol makes a major contribution to the lipid composition of a mammalian cell membrane. Therefore, to study the putative role played by cholesterol in the membrane interactions induced by Modelin-5-COOH and Modelin-5-$CONH_2$, monolayers were constructed with varying cholesterol levels in the presence of zwitterionic DMPC or DMPE (Figure 6). In the presence of DMPC:cholesterol monolayers regression analysis indicated there was a strong negative correlation between cholesterol levels and the pressure change induced for both Modelin-5-COOH (R^2 = 0.91) and Modelin-5-$CONH_2$ (R^2 = 0.96). Further statistical ANOVA analysis confirmed that there was a significant difference between the surface pressures in the presence of cholesterol for both Modelin-5-COOH [$F_{6,20}$ = 64.2; p = 0.00] and Modelin-5-$CONH_2$ [$F_{6,20}$ = 215.8; p = 0.00]. A similar negative linear relationship was also observed for Modelin-5-COOH (R^2 = 0.97) and Modelin-5-$CONH_2$ (R^2 = 0.96) where corresponding experiments were performed with monolayers in which PC had been substituted by PE. Again, ANOVA indicated that there was a significant difference in the mean surface pressure increase in the presence of cholesterol for both Modelin-5-COOH [$F_{6,20}$ = 383.9; p = 0.00] and Modelin-5-$CONH_2$ [$F_{6,20}$ = 868.5; p = 0.00]. Taken together, these data show that under the experimental conditions used here the presence of cholesterol inhibits the interaction of both Modelin-5 isoforms with the lipid systems tested.

Calcein Leakage Studies. Peptide-induced calcein relase assays were undertaken to investigate the lytic properties of the

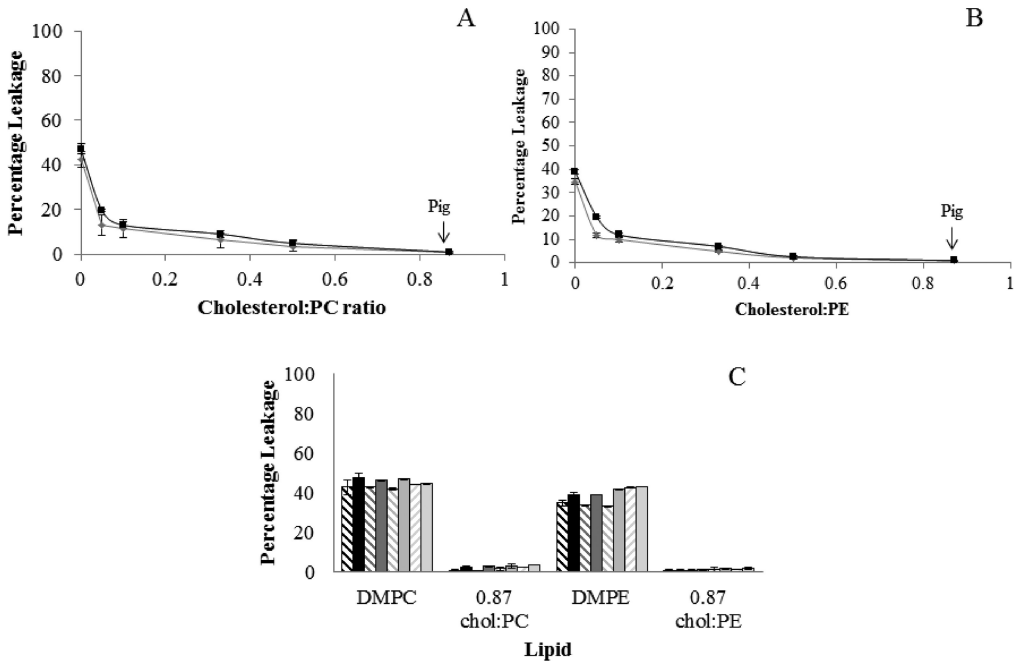

Figure 7. Effect of varying cholesterol levels on percentage calcein leakage in the presence of Modelin-5-COOH (gray) and Modelin-5-$CONH_2$ (black) for cholesterol:DMPC membranes (A) and cholesterol:DMPE membranes (B). (C) Percentage leakage for Modelin-5-COOH (striped) and Modelin-5-$CONH_2$ (solid) in the presence of DMPC, 0.87 Chol:PC, DMPE, and Chol:PE at temperatures 20 (black), 25 (dark gray), 50 (gray), and 55 °C (light gray). Error bars are standard deviations.

peptide isoforms. For vesicles formed from *E. coli* lipid extract (Table 1) Modelin-5-$CONH_2$ caused statistically significant greater levels of leakage (74%) compared to Modelin-5-COOH (42%) [$T = -17.71$; $p = 0.003$]. These data correlate with the MIC data, which showed that amidation of Modelin-5 enhanced its antimicrobial properties against *E. coli*. In comparison, a calcein leakage assay against vesicles formed from pig blood lipid extract showed Modelin-5-$CONH_2$ to caused only 2.6% leakage, whereas Modelin-5-COOH caused 0.72% leakage (Table 1). While these differences remain statistically significant [$T = -9.37$; $p = 0.011$] the levels of lysis remains low in both cases. When compared to the results from the hemolysis assay there is again a clear correlation between activity and the calcein release results.

The presence of cholesterol was also investigated within these systems. PC alone supported 42−47% leakage (Table 1) with data showing no statistically significant variation between the isoforms ($p > 0.05$). As the cholesterol to PC ratio increased from 0 to 0.87, mimetic of pig erythrocyte membrane, the percentage of calcein leakage decreased (Figure 7). Figure 7A shows that cholesterol containing DMPC vesicles are consistently more resistant to Modelin-5-COOH and Modelin-5-$CONH_2$ induced leakage, and ANOVA showed there was a significant difference in the mean calcein leakage in the presence of cholesterol for both peptides (Modelin-5-COOH [$F_{5,17} = 67.8$; $p = 0.00$] and Modelin-5-$CONH_2$ [$F_{5,17} = 391.2$; $p = 0.00$]). A similar trend was observed in the presence of cholesterol:PE vesicles (Figure 7B) where ANOVA again confirmed that there was a significant difference in the mean percentage calcein leakage in the presence of cholesterol for Modelin-5-COOH [$F_{5,17} = 572.1$; $p = 0.00$] and Modelin-5-$CONH_2$ [$F_{5,17} = 1834.30$; $p = 0.00$]. Further statistical analysis showed that in the presence of Modelin-5-COOH there was no significant difference observed in the percentage of calcein released in the presence of PE and PC cholesterol containing vesicles [$T = -1.9$; $p = 0.07$], indicating no preference for either lipid species. A similar results was also observed in the presence of Modelin-5-$CONH_2$ [$T = -0.84$; $p = 0.41$].

The effects of temperature on calcein release in the presence of DMPC:cholesterol or DMPE:cholesterol (ratio of 0.87) was investigated at 20, 25, 50, and 55 °C (Figure 7C). Statistical analysis showed there was no statistically significant difference in the mean calcein leakage over this temperature range for either peptide (Modelin-5-COOH [$F_{3,15} = 1.3$; $p = 0.32$] and Modelin-5-$CONH_2$ [$F_{3,15} = 1.0$; $p = 0.42$]). A similar result was observed with PE:cholesterol with temperature showing no statistically significant effect on leakage (Modelin-5-COOH [$F_{3,15} = 0.23$; $p = 0.87$] and Modelin-5-$CONH_2$ [$F_{2,11} = 0.87$; $p = 0.48$]).

Thermodynamic Analysis of Monolayer. In order to study the stability of the cholesterol:PC monolayer, compressibility modulus (C_s^{-1}) and the packing characteristics of cholesterol:PC were investigated using thermodynamic analysis. Compression isotherms were obtained from monolayers composed of cholesterol:PC at ratios of 0.05 and 0.1 in the presence and absence of each peptide (Figure 8). The results would suggest that cholesterol decreases the area per phospholipid molecule, and this is reflected in the compressibility modulus analysis C_s^{-1}, which showed that an increase in cholesterol increased the C_s^{-1} value in the absence of peptide (Table 2). The same trend was observed in the presence of peptide although the presence of Modelin-5-$CONH_2$ generated higher C_s^{-1} values than with the nonamidated isoform. The stability of the monolayers can be further investigated using the Gibbs's free energy of mixing (ΔG_{mix}) (Table 3). Negative values of ΔG_{mix} were observed for cholesterol:PC ratios in the absence of either peptide, indicating that the monolayers were thermodynamically stable. However, in the presence of either Modelin-5-COOH or Modelin-5-$CONH_2$, at surface pressures >20 mN m^{-1}, stability was reduced.

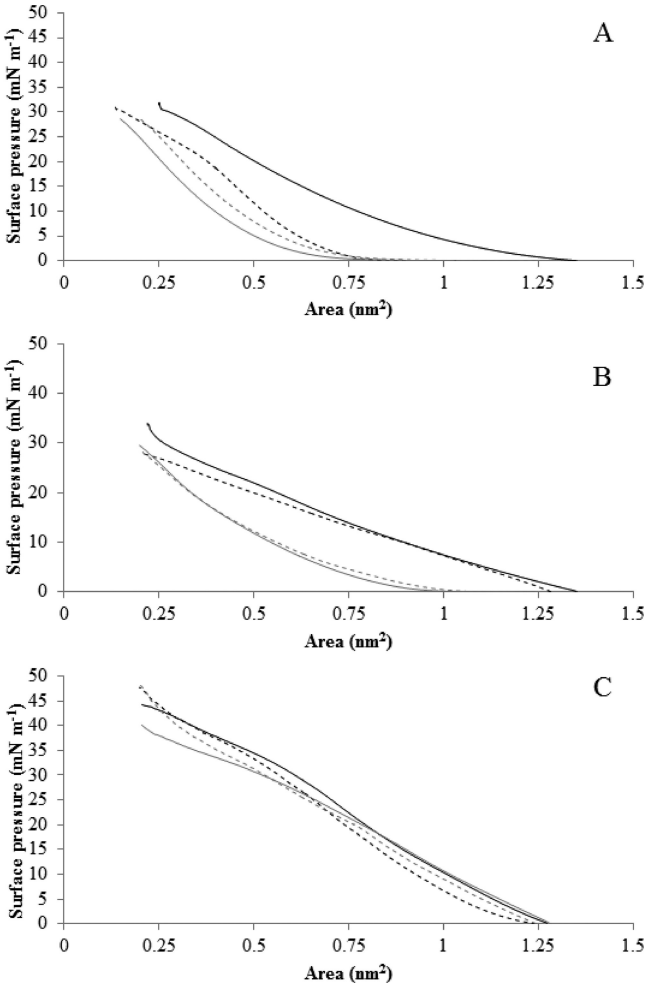

Figure 8. Compression isotherms derived from lipid mixtures that corresponded to membranes of DMPC (solid black), 0.05 cholesterol:PC (dotted black), 0.1 cholesterol:PC (dotted gray), and cholesterol (solid gray) in the absence (A) and presence of Modelin-5-COOH (B) and Modelin-5-CONH$_2$ (C).

Binding Properties. Previous studies have shown that in the presence of *E. coli* membranes Modelin-5 isoforms had binding coefficients of 9.6 μM (Modelin-5-COOH) and 10.1 μM (Modelin-5-CONH$_2$).[9] Since both peptides lack tryptophan residues, FPE, a fluorescent probe which has been extensively used to model peptide membrane binding,[41,44,45] was deployed to monitor their ability to bind to model membranes. The incorporation of FPE into cholesterol:PE lipid mix vesicles was checked using $CaCl_2$ and calcimycin (A23187) to determine which side of the membrane the probe was located. Figure 9A shows for each cholesterol:PE ratio the addition of Ca^{2+} ions to a suspension of FPE cholesterol:PE vesicles increases the fluorescence intensity, indicating that the probe is accessible in the external leaflet.[41] Following the addition of the ionophore, calcimycin (A23187), the fluorescence increased again by a third (Figure 9A), as the calcimycin enabled the Ca^{2+} to access the interior of the vesicle.[41] This is in line with other studies which have shown approximately $^1/_3$ of the probe is localized in the internal leaflet.[41] The peptides were then assayed for the ability to bind to PE vesicles containing varying amounts of cholesterol. Modelin isoforms show hyperbolic binding (Figure 9B,C) to FPE-labeled vesicles. Further analysis of the binding coefficients with these vesicles showed that in high cholesterol conditions (ratio 0.25) both peptides were able to bind to the membrane, but with K_d values of 32.17 for Modelin-5-COOH and 11.5 μM for Modelin-5-CONH$_2$ (Figure 9D). These values were 4−10 times higher in the absence of cholesterol where the K_d value was found to be 3.97 μM for Modelin-5-COOH and 3.21 μM for Modelin-5-CONH$_2$ showing that cholesterol had decreased binding efficiency. In addition, statistical analysis showed that there was no significant differences between the isoforms when binding cholesterol free vesicles [T = 3.34; p = 0.08], but the difference between the K_d value in the presence of cholesterol was significant [T = 49.78; p = 0.00], which would imply that cholesterol had a greater inhibitory effect on the nonamidated moiety.

DISCUSSION

The composition of cell membranes is known to be fundamental to the membrane interaction, activity, and selectivity of AMPs,[24,25,46] yet the mechanisms involved in the interaction between AMPs and prokaryotic versus eukaryotic cell membranes remain unclear. The variation in lipid−AMP interaction is known to depend upon the relative composition, stability, and lipid packing characteristics of the target cell membrane.[47,48] For example, reduced levels of DOPE in *Bacillus subtilis* and *E. coli* membranes are compensated for by a large increase in DOPG and CL, which is known to support a preference toward nonlamellar formation (H_{II} phase),[49] and AMPs have been shown to have varying efficacy against these two species with the membrane composition being a key determinant in activity. Furthermore, since the discovery of AMPs, bacteria such as *S. aureus* have developed resistance to AMPs[50] by adapting their membrane fluidity and membrane lipid composition,[51] further evidencing the importance of the lipid environment for AMP efficacy.

The behavior of Modelin-5 isoforms when coming in contact with prokaryotic cells has been previously investigated,[9] and a model has been proposed for membrane interaction. At the membrane interface the peptides which utilize a pore and/or carpet-type mechanism of action are generally unordered in solution[10,52] and fold to form an amphiphilic structure at the membrane interface (Figure 10).[10,52] At low peptide concentrations, AMPs lie parallel to the surface,[53] and above a certain peptide/lipid ratio they may adopt a more perpendicular

Table 2. Compressibility Modulus (C_s^{-1}, mN m^{-1}) for Modelin-5-COOH and Modelin-5-CONH$_2$

	absence of peptide		Modelin-5-COOH		Modelin-5-CONH$_2$	
π (mN m^{-1})	0.05 Chol:PC	0.1 Chol:PC	0.05 Chol:PC	0.1 Chol:PC	0.05 Chol:PC	0.1 chol:PC
10	25.6	32.9	26.9	27.1	41.4	43.9
15	25.9	30.2	21.6	21.9	41.4	46.5
20	24.3	24.8	17.3	17.6	36.3	44.4
25	20.6	20.9	13.3	13.5	28.9	39.1

dx.doi.org/10.1021/bi201267v | *Biochemistry* 2011, 50, 10898−10909

Table 3. Thermodynamics of Chol:PC 0.05 and 0.1[a]

	0.05			0.1		
π (mN m^{-1})	absence of peptide	Modelin-5-COOH	Modelin-5-CONH$_2$	absence of peptide	Modelin-5-COOH	Modelin-5-CONH$_2$
10	−3.7	0.0	−0.3	−3.1	−0.1	−0.8
15	−4.8	0.0	−0.4	−3.9	−0.1	−1.2
20	−5.9	−0.2	−0.6	−4.6	−0.2	−1.5
25	−6.6	−0.5	−0.8	−4.9	−0.6	−1.7

[a]The Gibbs free energy of mixing (ΔG_{mix}, J mol^{-1}) of lipid monolayers at varying surface pressure.

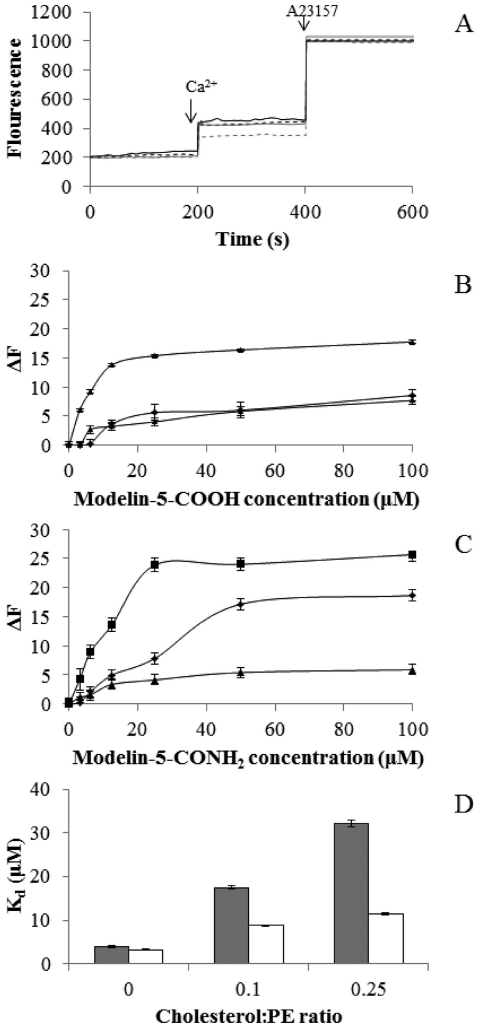

Figure 9. Incorporation of FPE into cholesterol:PE vesicles. (A) For each cholesterol:PE molar ratio (DMPE (solid dark gray), cholesterol:PE ratios 0.1 (dashed gray), 0.25 (solid black) and 0.33 (dashed black), fluorescence intensity was recorded at 490 nm in the absence of peptide. At 200 s 10 mM $CaCl_2$ was added to the system. After a further 200 s 3 μM A23157 ionophore was added. Binding curve for Modelin-5-COOH (B) and Modelin-5-CONH$_2$ (C) to FPE labeled cholesterol:PE DMPE (solid dark gray), cholesterol:PE molar ratios 0 (◆) 0.1 (■), and 0.25 (▲). F is fluorescence change in arbitrary units. (D) Binding coefficient (K_d) for Modelin-5-COOH (gray) and Modelin-5-CONH$_2$ (white) in the presence of cholesterol:PE ratios. Error bars are standard deviations.

orientation.[53,54] In this model efficacy is dependent upon the local concentration of the AMP, which in turn depends on its ability to bind and form a stable structure at the membrane interface.

At the membrane surface Modelin-5 isoforms are predicted to form an amphiphilic α-helical structure, which lies horizontal to the plane[9] and allows shallow penetration into the hydrophobic core of the lipid interior. This orientation would allow concentration of the peptide at the membrane interface leading to the lipid headgroups being pushed aside by the peptide, thereby forcing a gap to form in the hydrophobic region and breakdown of the membrane due to hydrophobic mismatch.[55] Hydrophobic mismatch is important in determining the orientation of a peptide in a membrane, where peptides may tilt their helices and the lipids may distort their acyl chains by stretching or compression to match with the peptide molecular architecture.[56] It has been shown that these initial stages of association are driven by amphiphilicity and dependent on hydrophobic grooves on the helix surface to drive activity.[57] A lack of stable association would therefore drive the peptide to dissociate from the membrane surface, thereby decreasing efficacy (Figure 10).

Increasing the level of cholesterol was seen to inhibit binding of both isoforms and would therefore indicate that cholesterol is having a protective effect by preventing insertion of the peptide into the membrane. This is supported by the CD analysis since the amphiphilic α-helical structure only forms at an asymmetric interface, and hence the decrease in helicity observed with increasing cholesterol levels indicates less peptide is associated with the lipid. This would be in line with studies on melittin which showed the presence of cholesterol reduced the efficiency of melittin pore formation by inhibiting membrane association.[29] There have been some reports that AMPs behave differently around the lipid phase transition temperature,[43,58] but both peptides tested showed statistically similar responses in the presence of PE (transition temperature 23 °C) and PC (transition temperature 50 °C), indicating this was not an influencing factor. Furthermore, both Modelin-5 peptide isoforms did not show any statistically significant change in structural conformation, and there was no change in calcein leakage over the temperature range 20−60 °C. The lack of temperature effect emphasizes the stability of these peptide−lipid associations once they have occurred.

The presence of cholesterol in mixed monolayers has been extensively studied because of its biological relevance and the nonideal mixing behavior.[59] Cholesterol plays a key role in the lipid order in membranes while helping maintain membrane fluidity.[60] Cholesterol also functions as a spacer molecule to compensate for the head−tail size mismatch in the lipid molecules and hence induces tighter packing of the lipid species. Indeed, it has previously been shown that the addition of cholesterol decreases the area per lipid hydrocarbon chain and increases the area compressibility modulus of the bilayer.[60] As the area per lipid hydrocarbon chain decreases due to tighter packing of membrane components, this would prevent the peptide penetrating the lipid headgroup region and lead to a decrease in the peptides exposure to the hydrocarbon surface.

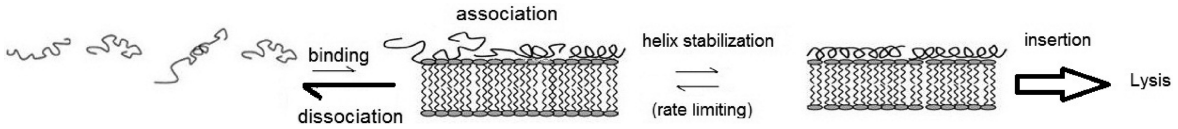

Figure 10. Schematic illustration of Modelin-5 peptide interacting with the membrane showing in the absence of cholesterol once the peptide binds to the membrane it could dissociate or form helical structure. The key driver for increased efficacy by amidation would therefore appear to be due to the enhanced stability of the helix at an asymmetric interface and the fact amidation can therefore help overcome a rate-limiting binding step in cell lysis. However, in the presence of cholesterol, the mechanism of interaction would move from binding to dissociation and hence no insertion into the membrane.

This would be predicted to decrease the hydrophobic attraction between the peptide and the membrane[60] and hence inhibit the stabilization of the peptide in the amphiphilic secondary arrangement required for activity. It is therefore not surprising that Table 2 shows that in the presence and absence of peptide the C_s^{-1} increases with increasing cholesterol concentration, which supports the view that cholesterol provides decreased opportunity for hydrophobic association and so decreases binding. Previous studies have shown[22] cholesterol, lanosterol, and ergosterol reduced the membrane binding of LL-37, but these authors showed no evidence of binding or inhibition for another AMP, Temporin L. While cholesterol levels therefore, appear to have decreased the efficiency of binding for both modelin isoforms, sterols do not consistently inhibit AMP activity. Indeed, in this study the impact of cholesterol was seen to be greater on the non-amidated peptide over the amidated isoform. In a membrane with reduced negative charge, the increase in binding of Modelin-5 to the membrane maybe compensated by the positive amidation charge on the N-terminus, enabling the peptide to tilt such that the hydrophobic side chains of the membrane are in line with the hydrophobic face of the helix and hence enabling interaction of the acyl chain region of the membrane. This greater level of engagement may support greater membrane binding for the amidated isoform, which would be indicative of the differences in K_d and higher levels of vesicle lysis seen with this peptide and hence explaining the differential effect of cholesterol on the isoforms.

In the present study, Modelin-5-$CONH_2$ showed increased helicity in the presence of *E. coli* lipid extract (Table 1) compared to the non-amidated isoform, which correlates with the monolayer studies which showed greater increases in surface pressure change in the presence of the amidated peptide compared to the non-amidated version (Figure 5A). This would be in line with amidation enhancing helical stability so enabling the helix once formed at the interface to engage in a more energetically favorable association driving the model toward binding and local concentration (Figure 10). Thermodynamic analysis into the packing characteristics of cholesterol:PC membranes shows that ΔG_{mix} was negative in the absence of peptide, indicating the membrane was thermodynamically stable (Table 3). Although in the presence of peptide ΔG_{mix} remained negative, the peptide did however have an overall destabilizing effect on the membrane as expected from peptide lipid penetrations.

An increase in cholesterol content to a ratio of 0.1 in the system further decreased the destabilization by the peptide, which would fit with the hypothesis that it prevents the peptide from mixing with the lipid system. This is supported by data where the depletion of cholesterol also increases the lytic activity of the two peptides (Figure 7) as the C_s^{-1} decreases (Table 2), supporting the notion that membrane-damaging activity of these peptides was attenuated by cholesterol and hence cholesterol-containing vesicles are more resistant to Modelin-5-induced permeabilization or lysis than cholesterol-free vesicles. Similar findings have been shown for β-sheet cationic AMPs, cateslytin,[61] which has a preference for fungal membranes over eukaryotic membrane. The primary role of the sterol in providing protection is further evidenced by the fact that we could find no differences between PC and PE lipid systems with the greatest impact on activity correlating solely with cholesterol levels.

In conclusion, the presence of cholesterol in the membrane increased packing density and appears to have prevented stable α-helical formation at the membrane interface so driving the model of peptide interaction toward dissociation as evidenced by the larger K_d values. This prevents local concentration of the peptide at the membrane interface and so inhibits activity.

Abbreviations

AMP, antimicrobial peptide; CD, circular dichroism; Chol, cholesterol; C_s^{-1}, compressibility modulus; DMPC, 1,2-dimyristoyl-*sn*-glycero-3-phosphocholine; DMPE, dimyristoyl-*sn*-glycero-3-phosphorylethanolamine; ΔG_{mix}, Gibbs free energy of mixing; K_d, binding coefficient; MIC, minimum inhibitory concentration; PBS, phosphate buffered saline; PC, phosphatidylcholine; PE, phosphatidylethanolamine; PI, phosphatidylinositol; PS, phosphatidylserine; RBC, red blood cells; SM, sphingomyelin; π, surface pressure.

AUTHOR INFORMATION

Corresponding Author

*Ph: +44 (0) 1772 892504. Fax: +44 (0) 1772 892936. E-mail: daphoenix@uclan.ac.uk.

REFERENCES

(1) Jacobs, M. R., Palavecino, E., and Yomtovian, R. (2001) Don't bug me: the problem of bacterial contamination of blood components--challenges and solutions. *Transfusion 41*, 1331−1334.

(2) Vasconcelos, E., and Seghatchian, J. (2004) Bacterial contamination in blood components and preventative strategies: an overview. *Transfus. Apher. Sci. 31*, 155−163.

(3) Goodnough, L. T., Shander, A., and Brecher, M. E. (2003) Transfusion medicine: looking to the future. *Lancet 361*, 161−169.

(4) Wainwright, M., Phoenix, D. A., Smillie, T. E., and Wareing, D. R. (2001) Phenothiaziniums as putative photobactericidal agents for red blood cell concentrates. *J. Chemother. 13*, 503−509.

(5) Rice, L., Wainwright, M., and Phoenix, D. A. (2000) Phenothiazine photosensitizers. III. Activity of methylene blue derivatives against pigmented melanoma cell lines. *J. Chemother. 12*, 94−104.

(6) Huston, B. M., Brecher, M. E., and Bandarenko, N. (1998) Lack of efficacy for conventional gamma irradiation of platelet concentrates to abrogate bacterial growth. *Am. J. Clin. Pathol. 109*, 743−747.

(7) Wainwright, M. (2000) Methylene blue derivatives--suitable photoantimicrobials for blood product disinfection? *Int. J. Antimicrob. Agents 16*, 381−394.

(8) Harris, F., Sayed, Z., Hussain, S., and Phoenix, D. A. (2004) An investigation into the potential of phenothiazinium-based photosensitisers to act as PDT agents. *Photodiagn. Photodyn. Ther. 1*, 231–239.
(9) Dennison, S. R., and Phoenix, D. A. (2011) Influence of C-terminal amidation on the efficacy of modelin-5. *Biochemistry 50*, 1514–1523.
(10) Shai, Y. (1999) Mechanism of the binding, insertion and destabilization of phospholipid bilayer membranes by alpha-helical antimicrobial and cell non-selective membrane-lytic peptides. *Biochim. Biophys. Acta 1462*, 55–70.
(11) Bessalle, R., Gorea, A., Shalit, I., Metzger, J. W., Dass, C., Desiderio, D. M., and Fridkin, M. (1993) Structure-function studies of amphiphilic antibacterial peptides. *J. Med. Chem. 36*, 1203–1209.
(12) Mor, A., and Nicolas, P. (1994) The NH2-terminal alpha-helical domain 1–18 of dermaseptin is responsible for antimicrobial activity. *J. Biol. Chem. 269*, 1934–1939.
(13) Hoskin, D. W., and Ramamoorthy, A. (2008) Studies on anticancer activities of antimicrobial peptides. *Biochim. Biophys. Acta 1778*, 357–375.
(14) Papo, N., Shahar, M., Eisenbach, L., and Shai, Y. (2003) A novel lytic peptide composed of DL-amino acids selectively kills cancer cells in culture and in mice. *J. Biol. Chem. 278*, 21018–21023.
(15) Dennison, S. R., Harris, F., Bhatt, T., Singh, J., and Phoenix, D. A. (2009) The effect of C-terminal amidation on the efficacy and selectivity of antimicrobial and anticancer peptides. *Mol. Cell. Biochem. 332*, 43–50.
(16) Dennison, S. R., Harris, F., Bhatt, T., Singh, J., and Phoenix, D. A. (2010) A theoretical analysis of secondary structural characteristics of anticancer peptides. *Mol. Cell. Biochem. 333*, 129–135.
(17) Salvioli, G., Gaetti, E., Panini, R., Lugli, R., and Pradelli, J. M. (1993) Different resistance of mammalian red blood cells to hemolysis by bile salts. *Lipids 28*, 999–1003.
(18) Belokoneva, O. S., Villegas, E., Corzo, G., Dai, L., and Nakajima, T. (2003) The hemolytic activity of six arachnid cationic peptides is affected by the phosphatidylcholine-to-sphingomyelin ratio in lipid bilayers. *Biochim. Biophys. Acta 1617*, 22–30.
(19) Nelson, G. J. (1967) Lipid composition of erythrocytes in various mammalian species. *Biochim. Biophys. Acta 144*, 221–232.
(20) Nelson, G. J. (1967) Composition of neutral lipids from erythrocytes of common mammals. *J. Lipid Res. 8*, 374–379.
(21) Sood, R., Domanov, Y., Pietiainen, M., Kontinen, V. P., and Kinnunen, P. K. (2008) Binding of LL-37 to model biomembranes: insight into target vs host cell recognition. *Biochim. Biophys. Acta 1778*, 983–996.
(22) Sood, R., and Kinnunen, P. K. (2008) Cholesterol, lanosterol, and ergosterol attenuate the membrane association of LL-37(W27F) and temporin L. *Biochim. Biophys. Acta 1778*, 1460–1466.
(23) Zhao, H., and Kinnunen, P. K. (2002) Binding of the antimicrobial peptide temporin L to liposomes assessed by Trp fluorescence. *J. Biol. Chem. 277*, 25170–25177.
(24) Zhao, H., Sood, R., Jutila, A., Bose, S., Fimland, G., Nissen-Meyer, J., and Kinnunen, P. K. (2006) Interaction of the antimicrobial peptide pheromone Plantaricin A with model membranes: implications for a novel mechanism of action. *Biochim. Biophys. Acta 1758*, 1461–1474.
(25) Mason, A. J., Marquette, A., and Bechinger, B. (2007) Zwitterionic phospholipids and sterols modulate antimicrobial peptide-induced membrane destabilization. *Biophys. J. 93*, 4289–4299.
(26) Alakoskela, J. M., Jutila, A., Simonsen, A. C., Pirneskoski, J., Pyhajoki, S., Turunen, R., Marttila, S., Mouritsen, O. G., Goormaghtigh, E., and Kinnunen, P. K. (2006) Characteristics of fibers formed by cytochrome c and induced by anionic phospholipids. *Biochemistry 45*, 13447–13453.
(27) Barman, H., Walch, M., Latinovic-Golic, S., Dumrese, C., Dolder, M., Groscurth, P., and Ziegler, U. (2006) Cholesterol in negatively charged lipid bilayers modulates the effect of the antimicrobial protein granulysin. *J. Membr. Biol. 212*, 29–39.
(28) Monette, M., Van Calsteren, M. R., and Lafleur, M. (1993) Effect of cholesterol on the polymorphism of dipalmitoylphosphatidylcholine/melittin complexes: an NMR study. *Biochim. Biophys. Acta 1149*, 319–328.
(29) Gomara, M. J., Nir, S., and Nieva, J. L. (2003) Effects of sphingomyelin on melittin pore formation. *Biochim. Biophys. Acta 1612*, 83–89.
(30) Oh, D., Shin, S. Y., Lee, S., Kang, J. H., Kim, S. D., Ryu, P. D., Hahm, K. S., and Kim, Y. (2000) Role of the hinge region and the tryptophan residue in the synthetic antimicrobial peptides, cecropin A(1–8)-magainin 2(1–12) and its analogues, on their antibiotic activities and structures. *Biochemistry 39*, 11855–11864.
(31) Song, Y. M., Park, Y., Lim, S. S., Yang, S. T., Woo, E. R., Park, I. S., Lee, J. S., Kim, J. I., Hahm, K. S., Kim, Y., and Shin, S. Y. (2005) Cell selectivity and mechanism of action of antimicrobial model peptides containing peptoid residues. *Biochemistry 44*, 12094–12106.
(32) Bligh, E. G., and Dyer, W. J. (1959) A rapid method of total lipid extraction and purification. *Can. J. Med. Sci. 37*, 911–917.
(33) Rose, H. G., and Oklander, M. (1965) Improved Procedure for the Extraction of Lipids from Human Erythrocytes. *J. Lipid Res. 6*, 428–431.
(34) Henzler Wildman, K. A., Lee, D. K., and Ramamoorthy, A. (2003) Mechanism of lipid bilayer disruption by the human antimicrobial peptide, LL-37. *Biochemistry 42*, 6545–6558.
(35) Forood, B., Feliciano, E. J., and Nambiar, K. P. (1993) Stabilization of alpha-helical structures in short peptides via end capping. *Proc. Natl. Acad. Sci. U. S. A. 90*, 838–842.
(36) Seeling, A. (1987) Local anesthetics and pressure: a comparison of dibucaine binding to lipid monolayers and bilayers. *Biochim. Biophys. Acta 899*, 196–204.
(37) Gennaro, R., and Zanetti, M. (2000) Structural features and biological activities of the cathelicidin-derived antimicrobial peptides. *Biopolymers 55*, 31–49.
(38) Demel, R. A. (1974) Monolayers--description of use and interaction. *Methods Enzymol. 32*, 539–544.
(39) Davies, J. T., and Rideal, E. K. (1963) *Interfacial Phenomena*, 2nd ed., Academic Press, New York.
(40) Todd, J. (1963) *Introduction to the Constructive Theory of Functions*, Academic Press, New York.
(41) Wall, J., Golding, C. A., Van Veen, M., and O'Shea, P. (1995) The use of fluoresceinphosphatidylethanolamine (FPE) as a real-time probe for peptide-membrane interactions. *Mol. Membr. Biol. 12*, 183–192.
(42) Owen, D. R. (2005) Short bioactive peptides, Helix BioMedix. Inc..
(43) Silvius, J. R. (1982) *Thermotropic Phase Transitions of Pure Lipids in Model Membranes and Their Modifications by Membrane Proteins*, John Wiley & Sons, Inc., New York.
(44) Hawrani, A., Howe, R. A., Walsh, T. R., and Dempsey, C. E. (2010) Thermodynamics of RTA3 peptide binding to membranes and consequences for antimicrobial activity. *Biochim. Biophys. Acta 1798*, 1254–1262.
(45) O'Toole, P. J., Morrison, I. E., and Cherry, R. J. (2000) Investigations of spectrin-lipid interactions using fluoresceinphosphatidylethanolamine as a membrane probe. *Biochim. Biophys. Acta 1466*, 39–46.
(46) Thennarasu, S., Tan, A., Penumatchu, R., Shelburne, C. E., Heyl, D. L., and Ramamoorthy, A. (2010) Antimicrobial and membrane disrupting activities of a peptide derived from the human cathelicidin antimicrobial peptide LL37. *Biophys. J. 98*, 248–257.
(47) Epand, R. M. (1997) Modulation of lipid polymorphism by peptides, in *Lipid Polymorphism and Membrane Properties* (Epand, R. F., Ed.) pp 237–252, Academic Press, San Diego, CA.
(48) Lohner, K., and Prenner, E. J. (1999) Differential scanning calorimetry and X-ray diffraction studies of the specificity of the interaction of antimicrobial peptides with membrane-mimetic systems. *Biochim. Biophys. Acta 1462*, 141–156.

(49) Dennison, S. R., Kim, Y. S., Cha, H. J., and Phoenix, D. A. (2008) Investigations into the ability of the peptide, HAL18, to interact with bacterial membranes. *Eur. Biophys. J. 38*, 37−43.
(50) Samuelsen, O., Haukland, H. H., Jenssen, H., Kramer, M., Sandvik, K., Ulvatne, H., and Vorland, L. H. (2005) Induced resistance to the antimicrobial peptide lactoferricin B in Staphylococcus aureus. *FEBS Lett. 579*, 3421−3426.
(51) Xiong, Y. Q., Mukhopadhyay, K., Yeaman, M. R., Adler-Moore, J., and Bayer, A. S. (2005) Functional interrelationships between cell membrane and cell wall in antimicrobial peptide-mediated killing of Staphylococcus aureus. *Antimicrob. Agents Chemother. 49*, 3114−3121.
(52) Shai, Y., and Oren, Z. (2001) From "carpet" mechanism to de-novo designed diastereomeric cell-selective antimicrobial peptides. *Peptides 22*, 1629−1641.
(53) Brogden, K. A. (2005) Antimicrobial peptides: pore formers or metabolic inhibitors in bacteria? *Nat. Rev. Microbiol. 3*, 238−250.
(54) Huang, H. W. (2000) Action of antimicrobial peptides: two-state model. *Biochemistry 39*, 8347−8352.
(55) Hallock, K. J., Lee, D. K., Omnaas, J., Mosberg, H. I., and Ramamoorthy, A. (2002) Membrane composition determines pardaxin's mechanism of lipid bilayer disruption. *Biophys. J. 83*, 1004−1013.
(56) Ramadurai, S., Holt, A., Schafer, L. V., Krasnikov, V. V., Rijkers, D. T., Marrink, S. J., Killian, J. A., and Poolman, B. (2010) Influence of hydrophobic mismatch and amino acid composition on the lateral diffusion of transmembrane peptides. *Biophys. J. 99*, 1447−1454.
(57) Dennison, S. R., Harris, F., and Phoenix, D. A. (2009) A study on the importance of phenylalanine for aurein functionality. *Protein Pept. Lett. 16*, 1455−1458.
(58) Jelokhani-Niaraki, M., Prenner, E. J., Kay, C. M., McElhaney, R. N., Hodges, R. S., and Kondejewski, L. H. (2001) Conformation and other biophysical properties of cyclic antimicrobial peptides in aqueous solutions. *J. Pept. Res. 58*, 293−306.
(59) Sabatini, K., Mattila, J. P., and Kinnunen, P. K. (2008) Interfacial behavior of cholesterol, ergosterol, and lanosterol in mixtures with DPPC and DMPC. *Biophys. J. 95*, 2340−2355.
(60) Chen, L. Y., Cheng, C. W., Lin, J. J., and Chen, W. Y. (2007) Exploring the effect of cholesterol in lipid bilayer membrane on the melittin penetration mechanism. *Anal. Biochem. 367*, 49−55.
(61) Jean-Francois, F., Desbat, B., and Dufourc, E. J. (2009) Selectivity of cateslytin for fungi: the role of acidic lipid-ergosterol membrane fluidity in antimicrobial action. *FASEB J. 23*, 3692−3701.

■ NOTE ADDED AFTER ASAP PUBLICATION

After this paper was published online November 21, 2011, the caption to Figure 9 was corrected. The revised version was published November 28, 2011.